Kaon photoproduction in the color-dielectric model

Dinghui Lu and Rubin H. Landau
Department of Physics, Oregon State University, Corvallis, Oregon 97331

Shashikant C. Phatak
Institute of Physics, Sachivalaya Marg, Bhubaneswar, India
(Received 15 May 1995)

The kaon photoproduction process $\gamma p \to K^+\Lambda$ is studied in a momentum-projected color dielectric quark model. In contrast to phenomenological analyses, only a few Feynman diagrams are used, yet the diagrams include form factors derived from quark wave functions. The predicted cross sections are close to experiment. The unitarization of the Born diagrams, which effectively includes the $K\Lambda$ final-state interaction, is found to be important in the prediction of the Λ polarization. It is concluded that only a small number of graphs is needed to explain the basic physics as long as a realistic model of the baryon structure and final-state interactions are included.

PACS number(s): 25.20.Lj, 12.39.Fe, 13.60.Le, 24.85.+p

I. INTRODUCTION

It has been known for some time [1,2] that the basic coupling constants $g_{K\Lambda p}$ and $g_{K\Sigma p}$ extracted from the study of kaon photoproduction, $\gamma p \to K^+\Lambda$, are inconsistent with the ones derived from KN scattering and $SU_F(3)$ symmetry. While this may indicate some interesting new physics, a more likely explanation is that the photoproduction and strong interaction calculations are not consistent with each other. Interestingly, although the underlying $SU(6)\times O(3)$ symmetry of the hadrons was established more than two decades ago [3] and has been used to predict KN scattering [4], there appears to be no published calculation of kaon photoproduction based directly on the quark model.

Most photoproduction calculations in the energy region near threshold ($E_\gamma = 0.911$ GeV) are variations of a phenomenological model which treats the baryons as structureless elementary particles [2,5], that is, with no form factors, and then includes a very large number of resonances. Unfortunately, no one resonance appears to dominate, and the number of parameters needing adjustment and the complexity of the calculation keep increasing with each new resonance. (In some approaches [6], the number of parameters per data point is reduced by application of crossing symmetry which permits the data from related processes to be described with a crossed version of the same theory.)

While these phenomenological models provide excellent fits to the data and are very useful when applied to hypernuclear photoproduction [7], their relation to the elementary strong interactions is not clear. Furthermore, the poor quality of the data, especially the lack of good polarization measurements, makes the final output of the nonlinear χ^2 search inconclusive [8]. In fact, the fitted elementary resonance parameters appear to change significantly as different data are included, and this leads to questions regarding the physical as well as statistical significance of the fitting. For example, the nonrelativistic quark models tells us that the $S_{11}(1650)$ resonance, which is needed in most of the phenomenological fitting, should not contribute at all if no eigenstate mixing occurs [9].

It is an experimental fact that hadrons have spatial extension and therefore cannot be described as point particles. Accordingly, Feynman diagrams which have only coupling constants at the hadronic vertices need to be generalized to include form factors which account for the composite nature of the particles. It is possible, then, that the discrepancy between the electromagnetic and hadronic coupling constants arises from the composite nature of the hadron not being included completely in the electromagnetic calculations. While a conclusive answer to this puzzle must await a complete theory of the hadronic interactions, it appears worthwhile to determine if a simple, yet fairly realistic, model of the hadronic interactions might provide even a basic description of the data.

In this paper we apply the chiral color dielectric model (CCDM) [10,11] to photoproduction. In this model, pseudoscalar mesons are introduced as elementary Goldstone bosons which preserve chiral symmetry. Baryons, however, are considered to be nonelementary composites of three relativistic quarks glued together and confined by the scalar average of the glueball field χ. As is true for other shell models of light systems, recoil and spurious motion of the center of mass are expected to be important corrections, yet are hard to include. We include them in the CCDM by use of the Peierls-Yaccoz projection method [12] (which limits us, for the moment, to the ground states of baryons).

Our photoproduction study is an extension of a previous CCDM investigation of the static properties of baryons and an investigation of scattering within the coupled πN-$\pi\Delta$ system. Both investigations have shown promising successes and we are encouraged to apply the model further. Accordingly, we keep the present calculation simple since we view it mainly as a feasibility study aimed to see how well a quark model with essentially no adjusted parameters can describe kaon photoproduction (the CCDM has parameters, but their

values are already fixed by these previous studies or by basic field theory).

II. MODEL

The connection of the color dielectric model to QCD was established many years ago [13]. The CCDM, which is closely related to the other nontopological soliton models [14,15], can be viewed as an improvement to the cloudy bag model. The $SU_F(3)$ version of the pseudovector-coupled CCDM Lagrangian at the quark level, up to $1/f$, is [10,11]

$$\mathscr{L}=\bar{q}\left[i\gamma^{\mu}\partial_{\mu}-\frac{m_q}{\chi}+i\frac{1}{2f}\gamma_5\gamma^{\mu}\lambda_a\cdot\partial_{\mu}\phi_a\right]q + \frac{\sigma_v^2}{2}(\partial_{\mu}\chi)^2-U(\chi)+\frac{1}{2}(\partial_{\mu}\phi_a)^2-\frac{1}{2}m_{\phi}^2\phi_a^2. \quad (1)$$

Here q, ϕ_a, and χ are the quark, pseudoscalar meson, and scalar glueball fields, respectively, λ_a are the SU(3) Gell-Mann matrices, and f is the average weak decay constant of the pseudoscalar meson octet. An important part of the Lagrangian (1) is the dielectric self-interaction field $U(\chi)$ which accounts for the average gluon field and produces a self-consistent, dynamic confinement of the quarks. Specifically, when we solve the equations of motion simultaneously for the dielectric field χ and the quark field q, the dielectric field vanishes along the physical perimeters of the baryons. This leads to the effective quark mass m_q/χ becoming infinite, and consequently to quark confinement. Left out of the Lagrangian (1) is the residual interaction of the gluons.

To calculate photoproduction we introduce a photon-quark interaction by taking the Lagrangian (1) and evoking the principle of minimal coupling:

$$\partial_{\mu}\rightarrow\partial_{\mu}-ieQA_{\mu}, \quad (2)$$

where A_{μ} is the photon field, e is the proton charge, and Q is the charge operator for a quark (q) or meson (ϕ_a). As discussed at length elsewhere [16], minimal coupling guarantees gauge invariance at the quark level. The resulting interaction Lagrangians are

$$\mathscr{L}'_{\gamma qq}=eQ\bar{q}\gamma^{\mu}qA_{\mu}, \quad (3)$$

$$\mathscr{L}'_{\gamma\phi\phi}=-ie(\phi_a^{\dagger}\cdot\partial^{\mu}\phi_a-\phi_a\cdot\partial^{\mu}\phi_a^{\dagger})A_{\mu}, \quad (4)$$

$$\mathscr{L}'_{qqK}=\frac{1}{2f}\bar{q}\gamma^{\mu}\gamma_5\lambda_a q\cdot\partial_{\mu}\phi_a, \quad (5)$$

$$\mathscr{L}^{\mathrm{SG}}=\frac{ie}{2f}\bar{q}\gamma^{\mu}\gamma_5\lambda_a q\cdot A_{\mu}\phi_a. \quad (6)$$

We use these Lagrangian to construct the hadronic-level vertex functions illustrated in Fig. 1. The construction consists of taking their matrix elements between momentum-projected baryon wave functions [11,15] and yields

$$H'_{\gamma BB'}(\vec{k})=-ie\sqrt{\frac{2\pi}{\omega_{\gamma}(k)}}u_{\gamma}(k)\mu_{B'B}\langle\chi_{B'}|\hat{\sigma}\cdot\hat{\epsilon}\times\hat{k}|\chi_B\rangle, \quad (7)$$

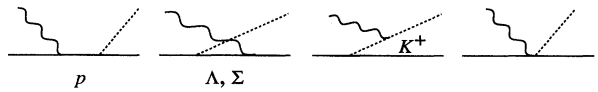

FIG. 1. The Feynman diagrams used to calculate the photoproduction reaction $\gamma p\rightarrow K^+\Lambda$. The solid line on the left of each diagram is a proton, while that on the right is a lambda. The wavy lines are photons and the dashed lines are mesons.

$$H'_{\gamma KK'}(\vec{q},\vec{q}',\vec{k})=\frac{2e(2\pi)^3\delta^3(\vec{q}'-\vec{q}+\vec{k})}{\sqrt{4\omega_K(q)\omega_K(q')}}\sqrt{\frac{2\pi}{\omega_{\gamma}(k)}}\vec{q}\cdot\hat{\epsilon}, \quad (8)$$

$$H'_{BB'K}(\vec{q})=\frac{i}{2f}\frac{I_{B'B}u_K(q)}{\sqrt{2\omega_K(q)}}\langle\chi_{B'}|\hat{\sigma}\cdot\vec{q}|\chi_B\rangle. \quad (9)$$

$$H^{\mathrm{SG}}(\vec{q},\vec{k})=\frac{ie}{2f}\sqrt{\frac{\pi}{\omega_{\gamma}(k)\omega_K(q)}}\langle\chi_{\Lambda}|[u_0(p)\hat{\sigma}\cdot\hat{\epsilon} - u_2(p)\hat{\sigma}\cdot\hat{p}\hat{\epsilon}\cdot\hat{p}]|\chi_p\rangle. \quad (10)$$

Here $\vec{k}$ and $\vec{q}$ are the momenta of the incoming photon and the outgoing kaon, and ω_{γ} and ω_K are the corresponding energies. The baryon spinors are denoted by χ_B and $\chi_{B'}$, $\hat{\sigma}$ is the Pauli spin operator, and $\mu_{B'B}$ are the magnetic moments of the baryons [which we calculate with SU(6) baryon wave functions [17]]. The factor $I_{B'B}$ in (9) contains SU(3) bare coupling constants for the explicit charge channels, for example, $I_{\Lambda p}=-3\sqrt{2}$ and $I_{\Sigma p}=-\sqrt{6}/3$. Finally, we have chosen the Coulomb gauge for the photon field so that $\epsilon_0=0$ and $\hat{k}\cdot\hat{\epsilon}=0$.

The new physics in our work arises from the form factors, u_{γ}, u_K, u_0, and u_2 in (7)–(10). These account for the composite nature of the baryons and provide convergence of the Feynman diagrams at large momentum transfers. In our model they are integrals over realistic (non-square-well) coordinate-space quark wave functions,

$$u_0(p)=N_s^2\int r^2dr\left[\left(g^2(r)-\frac{f^2(r)}{3}\right)j_0(pr) + \frac{2f^2(r)}{3}j_2(pr)\right], \quad (11)$$

$$u_2(p)=N_s^2\int r^2dr2f^2(r)j_2(pr), \quad (12)$$

$$u_{\gamma}(k)=N_s^2\int r^2dr2g(r)f(r)j_1(kr), \quad (13)$$

$$u_K(q)=N_s^2\int r^2dr\left[\left(g^2(r)-\frac{f^2(r)}{3}\right)j_0(qr) - \frac{4f^2(r)}{3}j_2(qr)\right], \quad (14)$$

where for clarity of presentation we give the expressions for static baryons. In these equations, $\vec{p}=\vec{q}-\vec{k}$ is the momentum

transfer, $g(r)$ and $f(r)$ are the upper and lower components of the quark wave function, and $j_l(kr)$ are spherical Bessel functions. In principle, the Dirac wavefunctions are different for light (u and d) quarks and strange quarks. However, earlier studies [10] have shown that the form factors do not depend much on the difference between these wave functions. We have therefore used light quark wave functions in the present calculation.

Once we have the interaction Hamiltonian, we calculate the transition matrix element at the tree level with the first- and second-order Born approximation

$$\langle f|T|i\rangle \simeq \langle f|H^{\rm SG}|i\rangle + \sum_n \frac{\langle f|H'|n\rangle\langle n|H'|i\rangle}{W-E_n}, \qquad (15)$$

where f, i, and n denote final, initial, and intermediate hadron states. Only the seagull graph $H^{\rm SG}$ of Fig. 1(d) contributes in first order, and only it survives at threshold. The second-order diagrams are calculated for the intermediate states shown in Figs. 1(a)– 1(c).

As must be, when all of the spin dependences of the interactions are substituted the resulting T matrix has the spin structure of the standard CGLN amplitude F [18,19]:

$$F = iF_1\hat{\sigma}\cdot\hat{\epsilon} + F_2\hat{\sigma}\cdot\hat{q}\,\sigma\cdot\hat{\epsilon}\times\hat{k} + iF_3\hat{\sigma}\cdot\hat{k}\hat{q}\cdot\hat{\epsilon} + iF_4\hat{\sigma}\cdot\hat{q}\hat{q}\cdot\hat{\epsilon}. \qquad (16)$$

Indeed, the CGLN amplitudes and our T's differ by only a normalization factor

$$F_i = (2\pi)^{-\frac{5}{2}}\sqrt{\frac{\omega_\gamma(k)E_p(k)\omega_K(q)E_\Lambda(q)}{W^2}}T_i, \qquad (17)$$

where W is the total c.m. energy, the T_i's are

$$T_1 = C(q)\left\{u_0(p) - \left[\frac{\mu_\Lambda I_{\Lambda p}}{W-E_\Lambda(P)-\omega_K(q)-k} + \frac{\mu_{\Sigma\Lambda}I_{\Sigma p}}{W-E_\Sigma(P)-\omega_K(q)-k}\right]qu_\gamma(k)u_K(q)2\hat{q}\cdot\hat{k}\right\}, \qquad (18)$$

$$T_2 = C(q)\left[\frac{\mu_p I_{\Lambda p}}{W-E_p(0)} + \frac{\mu_\Lambda I_{\Lambda p}}{W-E_\Lambda(P)-\omega_K(q)-k} + \frac{\mu_{\Sigma\Lambda}I_{\Sigma p}}{W-E_\Sigma(P)-\omega_K(q)-k}\right]qu_\gamma(k)u_K(q), \qquad (19)$$

$$T_3 = C(q)\left\{u_2(p) - \frac{kq}{\omega_K(p)}\frac{u_K(p)I_{\Lambda p}}{W-E_\Lambda(q)-\omega_K(q)-k} + \left[\frac{\mu_\Lambda I_{\Lambda p}}{W-E_\Lambda(P)-\omega_K(q)-k} + \frac{\mu_{\Sigma\Lambda}I_{\Sigma p}}{W-E_\Sigma(P)-\omega_K(q)-k}\right]2qu_\gamma(k)u_K(q)\right\}, \qquad (20)$$

$$T_4 = C(q)\left[-u_2(p) + \frac{q^2}{\omega_K(p)}\frac{I_{\Lambda p}u_K(p)}{W-E_\Lambda(q)-\omega_K(p)-k}\right], \qquad (21)$$

with a common factor $C(q) = (e/2f)\sqrt{\pi/k\omega_K(q)}$, and $\vec{P} = \vec{q} + \vec{k}$. The connection to the CGLN amplitudes is valuable since once the F_i's are known, all experimental observables are easily calculated. For example, the differential cross section for an unpolarized initial state is [19],

$$\frac{d\sigma}{d\Omega} = \frac{q}{k}\mathrm{Re}\{|F_1|^2 + |F_2|^2 - 2\cos\theta\, F_1^*F_2 + \sin^2\theta\,(\tfrac{1}{2}|F_3|^2 + \tfrac{1}{2}|F_4|^2 + F_1^*F_4 + F_2^*F_3 + \cos\theta\, F_3^*F_4)\}, \qquad (22)$$

where θ is the c.m. scattering angle. Likewise, the polarization of the Λ in the $\hat{k}\times\hat{q}$ direction is

$$P_\Lambda\frac{d\sigma}{d\Omega} = \frac{q}{k}\sin\theta\ \mathrm{Im}[-2F_1^*F_2 - F_1^*F_3 + F_2^*F_4 + \sin^2\theta\, F_3^*F_4 + \cos\theta\,(F_2^*F_3 - F_1^*F_4)]. \qquad (23)$$

The quark wave functions $f(r)$ and $g(r)$ and the scalar glueball field χ are determined simultaneously by solving self-consistently [11] the equation of motion deduced from the CCDM Lagrangian (1). We calculate the CCDM vertex functions using momentum-projected baryon states in the Breit frame. Note that when we calculate amplitudes, we explicitly break the elementary $SU_F(3)$ symmetry by using physical particle masses and by using the physical magnetic moments. We use the same parameters for the self-interaction scalar field χ and the same quark masses as used in the earlier study of the static properties of baryons [10]. The glueball mass $m_{\rm GB}$ is taken as 1 GeV (the mass of the lowest glueball candidate) and the kaon weak decay constant f_K is set equal to the pion weak decay constant, $f_\pi = 93$ MeV. As shown in the figures, we investigate the sensitivity of our results to a slight variation of these latter two constants.

Since we do not assume complex energies for the intermediate masses in our Born amplitudes, or dress them with multiple scatterings, the resulting CGLN amplitudes F_i's are real. Consequently the Λ polarization is predicted to be zero. To make our Born amplitudes more realistic, and to include some final-state interactions, we impose a unitarity constraint which also has the effect of producing complex amplitudes. We assume a two-channel problem in which our Born amplitude V is considered [20] as an approximation to the reaction matrix K:

$$V \simeq \begin{pmatrix} 0 & M_{\gamma K} \\ M_{\gamma K} & \tan\delta \end{pmatrix} \simeq K. \qquad (24)$$

Here the upper diagonal element is for γp elastic scattering and we approximate it as zero because of the weakness of a pure electromagnetic interaction relative to a strong one. The lower diagonal element is the $K^+\Lambda$ elastic scattering reaction matrix expressed in terms of the elastic phase shift δ. The off-diagonal elements are the multipoles of the transition matrix for the $\gamma p \to K^+\Lambda$ reaction [19], and we take them as

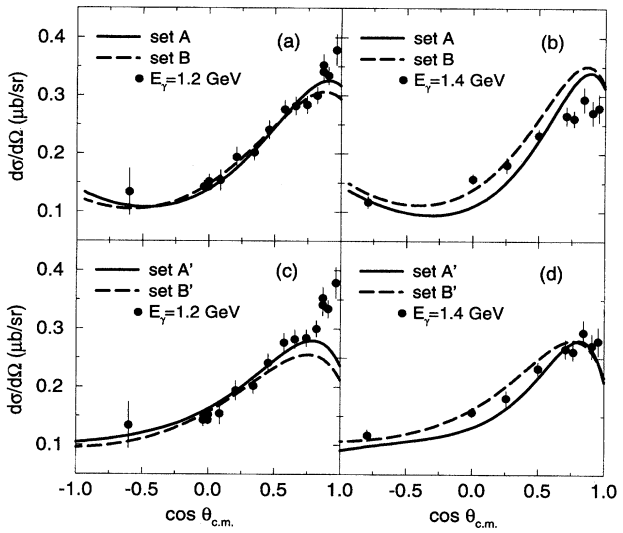

FIG. 2. The $\gamma p \to K^+\Lambda$ differential cross sections at $E_\gamma = 1.2$ and 1.4 GeV as a function K^+ scattering angle. Top, without the $K^+\Lambda$ final-state interaction; bottom, with the final-state interaction. The solid and dashed curves show the sensitivity to a $\sim 10\%$ variation in the values used for the kaon weak decay constant f_K and the glueball mass $m_{\rm GB}$.

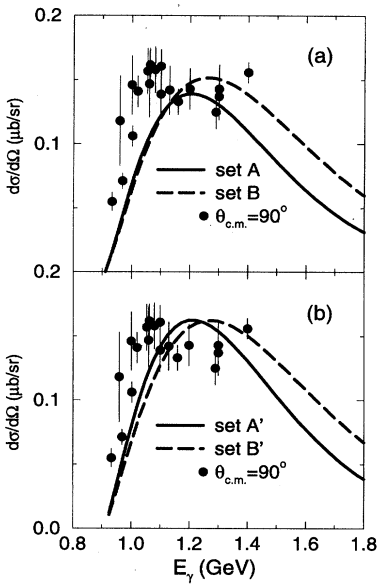

FIG. 3. The $\gamma p \to K^+\Lambda$ differential cross sections at 90° as a function of photon energy. Top, without the $K^+\Lambda$ final-state interaction; bottom, with the final-state interaction. The solid and dashed curves show the sensitivity to a $\sim 10\%$ variation in f_K and $m_{\rm GB}$.

equal for the on-shell K matrix. The transition matrix T is related to the reaction matrix via

$$T = K + iKT \tag{25}$$

$$\Rightarrow T = \begin{pmatrix} 0 & M_{\gamma K} e^{i\delta}\cos\delta \\ M_{\gamma K} e^{i\delta}\cos\delta & e^{i\delta}\sin\delta \end{pmatrix}. \tag{26}$$

It is clear from (26) that the off-diagonal elements now describe the $\gamma p \to K^+\Lambda$ reaction with corrections for $K^+\Lambda$ elastic scattering, that is, for final-state interactions. A problem with the application of (26) is that it requires us to know the $K^+\Lambda$ phase shifts, which have yet to be deduced from experiment. Accordingly, we use the K^+n phase shifts [21] as an approximation to the $K^+\Lambda$ phases [22].

III. RESULTS

In Fig. 2 we show the experimental data [23] and predicted differential cross sections for $\gamma p \to K^+\Lambda$ at $E_\gamma = 1.2$ and 1.4 GeV. In Fig. 3 we show the 90° differential cross section (the excitation function) as a function of energy. The upper parts of these figures do not include the $K^+\Lambda$ final-state interaction, while the bottom parts do. In the top part of Fig. 4 we show the predicted polarization at 1.1 GeV as a function of angle. In the bottom part of Fig. 4 we show the predicted Λ polarization at 90° as a function of energy.

In Figs. 2–4, the solid and dashed curves (set A vs B) show the sensitivity of the predictions to a $\sim 10\%$ variation of the kaon decay constant f_K and the glueball mass $m_{\rm GB}$.[1] This represents an acceptable range of variation of these model parameters as found in previous field-theory and CCDM calculations. Since these figures show no qualitative differences arising from these variations, the predictions we show may be considered as being made with no adjustable parameters.

We see in Fig. 2 that there is respectable agreement with all the differential cross section data. There is better agreement at 1.2 GeV than at 1.4 GeV, with the predicted forward-angle cross sections tending to be smaller than the data. The same trend is observed in the phenomenological analyses, leading us to believe that a modern measurement of these data may be valuable. We note, however, that the forward-angle cross sections are decreased by the inclusion of final-state interactions to the point where all of the 1.4 GeV data fall within the band of theoretical predictions. Although our model for final-state interactions is rather simple, we expect the trend to be general.

The predicted excitation functions shown in Fig. 3 follow the trend and magnitude of the data well, being below the data for energies below $E_\gamma = 1.2$ GeV, and falling off gradually beyond ~ 1.3 GeV. It is interesting to note in this regard that the phenomenological calculations require the addition of a good number of resonances at different energies to obtain an excitation function which does not fall off rapidly as a function of energy, while our calculation with only a few diagrams does not exhibit a rapid falloff with energy. The

[1]Explicitly, set A has $(m_{\rm GB}, f_K) = (900,90)$ MeV, set B has (1000,100) MeV, set A' has (900,70) MeV, and set B' has (1000,80) MeV.

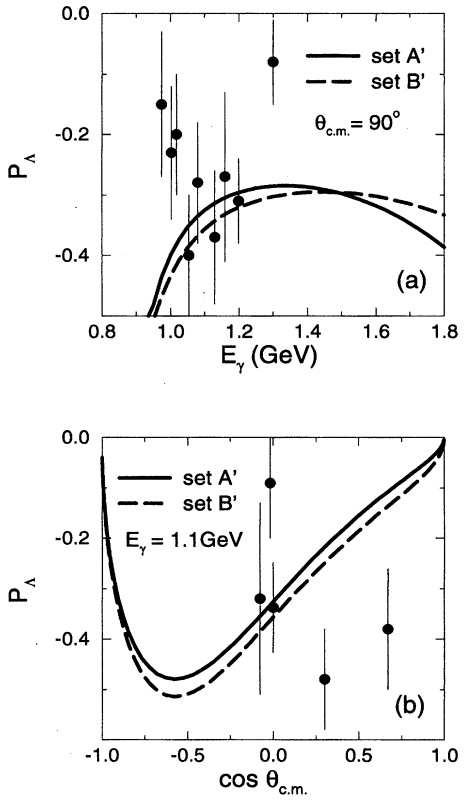

FIG. 4. Top, the Λ polarization at 90° as a function of photon energy; bottom, the angular dependence of P_Λ at $E_\gamma = 1.1$ GeV as a function of kaon scattering angle.

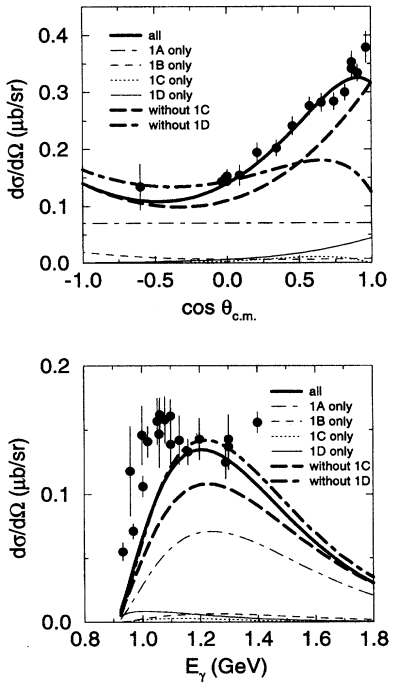

FIG. 5. The contributions of individual Feynman diagrams to the cross sections. Top, the differential cross section at $E_\gamma = 1.2$ GeV; bottom, the excitation function at $\theta_{\text{c.m.}} = 90°$.

difference apparently arises from our use of form factors derived from quark wave functions. The sensitivity of these 90° cross sections to final-state interactions does not appear high, yet at higher energies there is a significant sensitivity to model parameters.

The predicted Λ polarization in Fig. 4 is highly sensitive to final-state interactions (they are identically zero without them in our Born approximation calculations). The predicted polarizations have the right magnitude, but detailed comparisons may not be meaningful with such large experimental errors. In any case, polarization is sensitive to the details of calculation and we expect that improved agreement with the data will require the inclusion of resonances in the t and s channels and a proper calculation of final-state interactions.

Finally, in Fig. 5 we show the individual contribution of each Feynman diagram to the cross section. Clearly none of the diagrams dominates and the differential cross section is built up from a coherent sum of Figs. 1(a)–1(d) (the exception being threshold where only the seagull diagram survives). At $E_\gamma = 1.2$ GeV, the s-channel diagram contributes the most, whereas the seagull term still makes a significant contribution to the forward-angle differential cross section. In general, although no individual diagram dominates, they all add coherently and each makes a significant contribution.

IV. CONCLUSION

We have studied the kaon photoproduction process $\gamma p \to K^+\Lambda$ in a momentum-projected color dielectric quark model. We have used only a few Feynman diagrams (by contemporary standards), and use model parameters determined in previous work. We find that the predicted cross sections are close to experiment and that the $K^+\Lambda$ final-state interaction is crucial to predict the Λ polarization. We conclude that the spatial extension of the baryons, as included by our use of quark wave functions, is important in describing kaon photoproduction. Reproduction of the unpolarized data of the differential cross section does not require any explicit, intermediate resonances. This implies that these data cannot constrain the values of the coupling constants $g_{K\Lambda p}$ and $g_{K\Sigma p}$ effectively, and are not very useful for deducing the properties of N^* and Y^* resonances. The polarization appears sensitive to the $K\Lambda$ final-state interaction which needs to be included more accurately in the future as do explicit t- and s-channel resonances.

ACKNOWLEDGMENTS

We gratefully acknowledge support from the U.S. Department of Energy under Grant No. DE-FG06-86ER40283 at Oregon State University. We would like to thank Prof. S.R. Cotanch, Prof. V.A. Madsen, and Prof. A.W. Stetz for many helpful discussions and suggestions. S.C.P. would like to thank the Physics Department, Oregon State University for their warm hospitality and support, and R.H.L. would like to thank the Institute of Physics, Bhubaneswar, for their generous hospitality and support.

[1] A. S. Rosenthal, D. Halderson, K. Hodgkinson, and F. Tabakin, Ann. Phys. (N.Y.) **184**, 33 (1988); J. Cohen, Int. J. Mod. Phys. A **4**, 1 (1989).
[2] R. A. Adelseck and B. Saghai, Phys. Rev. C **42**, 108 (1990); R. A. Adelseck, C. Bennhold, and L. E. Wright, *ibid.* **32**, 1681 (1985).
[3] L. A. Copley, G. Karl, and E. Obryk, Nucl. Phys. **B13**, 303 (1969); R. P. Feynman, M. Kislinger, and F. Ravndal, Phys. Rev. D **3**, 2706 (1971).
[4] E. A. Veit, B. K. Jennings, A. W. Thomas, and R. C. Barrett, Phys. Rev. C **31**, 1033 (1985); E. A. Veit, A. W. Thomas, and B. K. Jennings, *ibid.* **31**, 2242 (1985).
[5] R. L. Workman, Phys. Rev. C **39**, 2456 (1989).
[6] C. R. Ji and S. R. Cotanch, Phys. Rev. C **38**, 2691 (1988); R. A. Williams, C. R. Ji, and S. R. Cotanch, *ibid.* **46**, 1617 (1992).
[7] S. S. Hsiao and S. R. Cotanch, Phys. Rev. C **28**, 1668 (1983).
[8] R. L. Workman, Phys. Rev. C **44**, 552 (1991).
[9] F. E. Close, *An Introduction to Quarks and Partons* (Academic Press, London, 1979).
[10] S. Sahu and S. C. Phatak, Mod. Phys. Lett. A **7**, 709 (1992); S. Sahu, Ph.D. thesis, Uktal University, Bhubaneswar, 1993.
[11] D. Lu, S. C. Phatak, and R. H. Landau, Phys. Rev. C **51**, 2207 (1995).
[12] R. E. Peierls and J. Yoccoz, Proc. Phys. Soc. London A **70**, 381 (1957).
[13] H. B. Nielsen and A. Patkos, Nucl. Phys. **B195**, 137 (1982); G. Chanfray, O. Nachtmann, and H. J. Pirner, Phys. Lett. **B147**, 249 (1984).
[14] A. G. Williams and L. R. Dodd, Phys. Rev. D **37**, 1971 (1988); A. W. Thomas, Adv. Nucl. Phys. **13**, 1 (1984).
[15] L. Wilets, *Non-Topological Solitons* (World Scientific, Singapore, 1989).
[16] M. Guidry, *Gauge Field Theories* (John Wiley & Sons, New York, 1991).
[17] W. M. Gibson and B. R. Pollard, *Symmetry Principles in Elementary Particle Physics* (Cambridge University Press, London, 1976).
[18] G. F. Chew, M. L. Goldberger, F. E. Low, and Y. Nambu, Phys. Rev. **106**, 1345 (1957); M. Gourdin and J. Dufour, Nuovo Cimento **27**, 1410 (1963).
[19] H. Thom, Phys. Rev. **151** 1322 (1966); J. S. Ball, *ibid.* **124**, 2014 (1961).
[20] M. Gell-Mann and K. M. Watson, Annu. Rev. Nucl. Sci. **4**, 219 (1954); M. L. Goldberger and K. M. Watson, *Collision Theory* (John Wiley & Sons, New York, 1964).
[21] R. A. Arndt *et al.*, Report No. WWW link: http://clsaid.phys.vt.edu/, 1995.
[22] J. J. J. Kokkedee, *The Quark Model* (W. A. Benjamin, New York, 1969).
[23] For a compilation of the kaon photoproduction data, see Ref.[2] and references therein.